

Raman-scattering study of exciton-phonon coupling in PbS nanocrystals

Todd D. Krauss and Frank W. Wise

Department of Applied Physics, Cornell University, Ithaca, New York 14850

(Received 6 November 1996)

The exciton-phonon coupling strength of PbS nanocrystals that strongly confine both charge carriers is investigated using resonant Raman scattering. The strength of this coupling (Huang-Rhys parameter $S \sim 0.7$) is four orders of magnitude greater than that predicted theoretically for the intrinsic states of the nanocrystal, but is the same order of magnitude as that measured for Cd(S,Se) nanocrystals. The large exciton-phonon coupling is consistent with one charge carrier being localized at the surface of the nanocrystal. [S0163-1829(97)11216-4]

I. INTRODUCTION

Semiconductor nanocrystals, also known as quantum dots, have been studied quite extensively recently due to their interesting physical properties and potential usefulness for applications. The electron and hole radii are each ~ 10 nm in PbS, and the Bohr radius (a_B) of the exciton is ~ 20 nm, so PbS nanocrystals offer unique opportunities for achieving strong quantum confinement of both charge carriers individually as well as the exciton. Quantum dots in the strong-confinement regime are expected to have greatly enhanced linear and nonlinear optical properties relative to the bulk materials. The sparse electronic spectra and easy access to the strong confinement regime make nanocrystals of the lead salts excellent candidate materials for device applications, such as optical switching. However, any benefits of strong quantum confinement are offset by significant broadening of the electronic transitions. Since the dominant source of homogeneous line broadening is expected to be coupling of electronic charge to the vibrational modes of the nanocrystal,¹ knowledge of the exciton-phonon interaction is critically important. Thus, in addition to its fundamental interest, the issue of exciton-phonon coupling has a bearing on the future utility of semiconductor nanocrystals.

Previous experimental studies of exciton-phonon coupling in semiconductor nanocrystals generally show little agreement with theory or each other, except for the order of magnitude of the coupling. Schmitt-Rink, Chemla, and Miller argued that based on charge neutrality the polar coupling of the exciton to phonons via the Fröhlich interaction should vanish as the radius of the nanocrystal decreases.¹ However, they also predict that nonpolar coupling to short-wavelength phonons will increase. More recent calculations, which account for valence-band degeneracy and conduction-band nonparabolicity in II-IV materials, predict an exciton-phonon coupling strength one to two orders of magnitude smaller than that for bulk materials.^{2,3} While the calculations generally agree that the exciton-phonon coupling strength is reduced in the nanocrystal relative to the bulk, they disagree regarding the trend in coupling strength with nanocrystal size. Some calculations²⁻⁴ predict an increase in exciton-phonon coupling strength as the nanocrystal radius is made smaller, while other calculations predict no change in the

coupling strength with nanocrystal radius.⁵ The measured values of the exciton-phonon coupling strength are one to two orders of magnitude greater than values calculated using the intrinsic exciton wave functions.⁵⁻⁹ These measurements more closely agree with calculations that include an additional charge,^{2,3} or use a donorlike exciton model appropriate for nanocrystals made with II-VI materials.⁴ Measurements of the exciton-phonon coupling strength as a function of nanocrystal size have produced widely varying results. Decreasing,⁶ increasing,^{8,9} and constant exciton-phonon coupling⁵ have all been found as the nanocrystal size is reduced.

Here we report an investigation of the electron-phonon coupling strength in PbS nanocrystals. Using resonant Raman spectroscopy, we determined the Huang-Rhys parameter of PbS nanocrystals 1.5 nm in radius ($R/a_B < 0.1$) to be $S \sim 0.7$. Using a displaced harmonic oscillators model, we accurately fit the resonance Raman excitation profile and account for the observed variation in the ratio of overtone to fundamental scattering with excitation wavelength. The measured coupling is four orders of magnitude larger than the value our calculation predicts, but is similar to values measured for other semiconductor nanocrystals.

By themselves, the electronic and vibrational properties of PbS nanocrystals possess interesting characteristics. Since these are not well known, they will be summarized briefly. The conduction and valence bands of bulk PbS are nondegenerate, and have nearly equal effective masses, so the bulk electron and hole wave functions are nearly identical. Using an effective mass model that neglects interband coupling, the wave functions are identical in the quantum dot. Using a four-band envelope-function formalism, the correct electronic structure of PbS nanocrystals was recently determined.¹⁰ The wave functions and energies were determined by starting with an accurate model of the band structure of the bulk material that accounts for interband coupling and the symmetry of the band-edge Bloch functions. The parameters of the model are all obtained from experiments on the bulk material, and the specific values are summarized in Ref. 10. Inclusion of the interband coupling results in electron and hole wave functions that are similar but not identical.¹⁰ The vibrational modes of PbS nanocrystals were also recently determined using resonant-Raman and far-

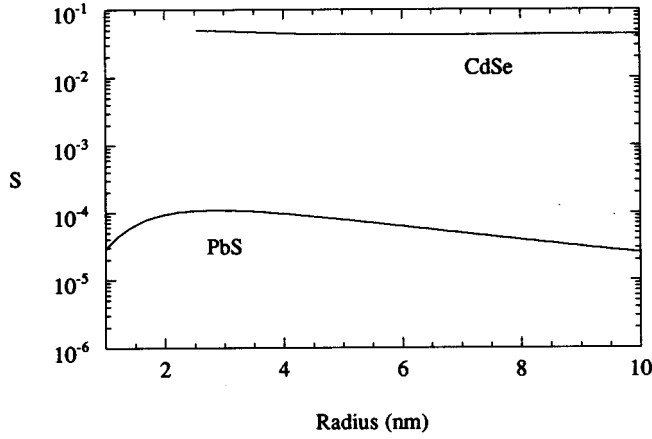


FIG. 1. Calculated size dependence of the Huang-Rhys parameter S for PbS and CdSe nanocrystals vs radius. The curve for CdSe was reproduced from Ref. 2. The coupling strength of CdSe has a minimum at a radius of ~ 7 nm.

infrared absorption spectroscopies.¹¹ The optically active vibrational modes of PbS nanocrystals generally have mixed longitudinal and transverse character. However, in resonant Raman scattering via the Fröhlich interaction, the observable modes have phonon angular momentum $l_p=0$ for excitation resonant with the lowest exciton state. These modes are purely radial (i.e., longitudinal) and have eigenfunctions similar to $l_p=0$ longitudinal optic (LO) vibrational modes previously obtained using dielectric theories.^{2,5} A more detailed discussion of the electronic and vibrational properties of PbS nanocrystals can be found in Ref. 10 and Ref. 11, respectively.

The electron-phonon coupling strength, via the Fröhlich interaction, is proportional to the net charge density in the nanocrystal. For PbS nanocrystals, the nearly identical electron and hole wave functions lead to overall charge neutrality. Thus the Huang-Rhys parameter S , a measure of the exciton-phonon coupling strength, is expected to be very small. S is given by^{2,5,12}

$$S = \sum_k \frac{1}{(\hbar \omega_p)^2} |V_{lm}(k)|^2, \quad (1)$$

where for phonon modes with $l_p=0$,

$$V_{00}(k) = f_{00}(k) \int e[|\psi_e(\mathbf{r})|^2 - |\psi_h(\mathbf{r})|^2] j_0(kr) Y_{00}(\theta, \phi) d^3r, \quad (2)$$

and

$$f_{00}(k)^2 = \frac{2\pi\hbar\omega_p}{k^2} \left(\frac{1}{\varepsilon_\infty} - \frac{1}{\varepsilon_0} \right) \frac{2}{R^3} \frac{1}{j_1^2(kR)}.$$

In the above equations, ε_∞ is the high-frequency dielectric constant, ε_0 is the static dielectric constant, R is the radius of the nanocrystal, ω_p is the frequency of the phonon mode with $l_p=0$, ψ_e and ψ_h are the wave functions of the electron and hole, respectively, and the sum is over all phonon wave vectors \mathbf{k} . Although the above expression for S is appropriate for a free-standing boundary condition, the same results are

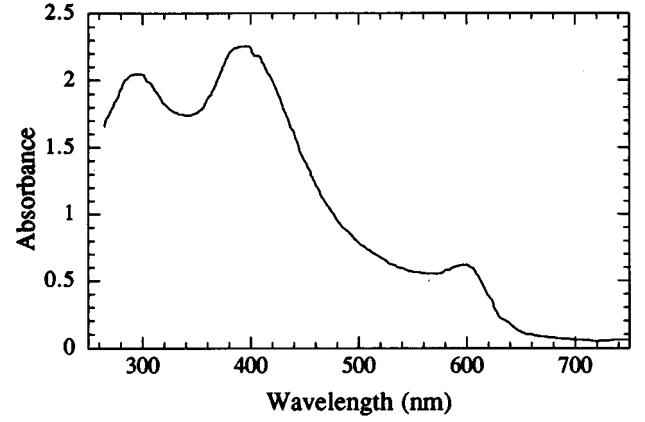


FIG. 2. Room-temperature absorption spectrum of PbS nanocrystals of radius 1.5 nm.

obtained if a rigid boundary condition is used.² Figure 1 shows a calculation of the Huang-Rhys parameter S for PbS quantum dots as a function of nanocrystal radius using the exciton wave functions calculated in Ref. 10 and the $l_p=0$ radial vibrational modes from Ref. 11. The nearly identical electron and hole masses in the bulk are responsible for the small value of the coupling at very large radius. As the radius decreases, coupling between the conduction and valence band leads to an increase in exciton-phonon coupling strength. At still smaller values of the radius, the confinement of the exciton is so strong that the exciton-phonon coupling decreases due to local charge neutrality. Small variations in the parameters used to model the band structure do not affect the conclusions regarding the size of the coupling, and the trend versus nanocrystal radius. In particular, variation of the electron or hole mass ratio by $\pm 10\%$ changes the result by less than 3×10^{-4} . For comparison, a similar calculation (reproduced from Ref. 2) for nanocrystals of a typical II-VI material, CdSe, is also shown. The calculated exciton-phonon coupling in PbS quantum dots is over 2 orders of magnitude smaller than the value for CdSe quantum dots at all radii. It is also interesting to note that the trend with nanocrystal radius is very different. In CdSe the coupling reaches a minimum at a radius of ~ 7 nm, and then increases with decreasing size due valence-band mixing.²

II. EXPERIMENTS AND RESULTS

The exciton-phonon coupling in PbS semiconductor nanocrystals stabilized by poly(vinyl alcohol) (PVA) was studied with resonance Raman spectroscopy. We synthesized PbS nanocrystals in an aqueous solution of PVA following the procedure in Ref. 13 and subsequently dried the colloid into thin films.¹⁴ The nanocrystal size was determined from images taken with a scanning transmission electron microscope (STEM), and by comparing the measured absorption spectra, shown in Fig. 2 with a calculated spectrum.¹⁰ The average radius is 1.5 nm, with a distribution in size of $\pm 4\%$. All three peaks in the absorption spectrum are in agreement with the wavelengths of the three lowest exciton transitions calculated for particles of 1.5 nm radius. A systematic comparison of the effect of nanocrystal size on electron-phonon coupling for PbS would be interesting. However, the fabrication of monodisperse PbS quantum dots with well-

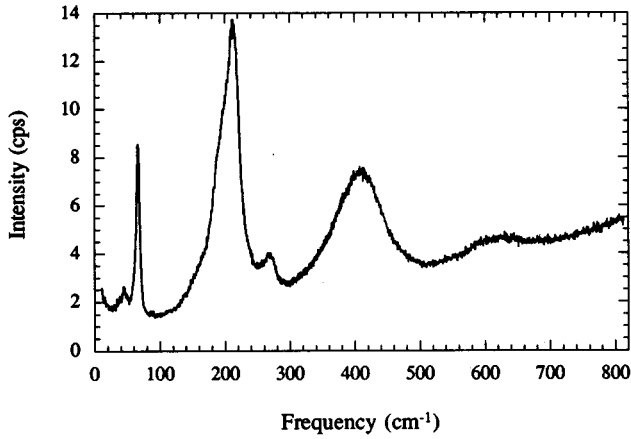


FIG. 3. Resonant Raman spectrum of 1.5-nm PbS nanocrystals recorded at 4.2 K with excitation at 584 nm. Similar spectra were obtained for other excitation wavelengths resonant with the lowest exciton state. The slight slope of the baseline is due to a luminescence background.

controlled but variable particle size in a polymer host has not been reported.

We recorded resonance Raman spectra in backscattering geometry with a Dilor model *xy* spectrometer, using a tunable dye laser (Rhodamine 590) and a HeNe laser for excitation. Spectra were recorded at 4.2, 77, and 300 K, with a resolution of 2.5 cm^{-1} , for various wavelengths across the lowest-energy exciton resonance. The range of excitation wavelengths was limited by the tunability of the dye laser. Each Raman spectrum was corrected for the spectral response of the spectrometer and also for effects of absorption in the sample.¹⁵ A typical spectrum is shown in Fig. 3. All of the spectra have a large peak at $\sim 215 \text{ cm}^{-1}$, with a reproducible shoulder at 190 cm^{-1} . Spectra recorded with excitation wavelengths between 573 and 610 nm show a broad overtone peak at $\sim 415 \text{ cm}^{-1}$. The intensity of this peak is strongly dependent on the excitation wavelength. For excitation wavelengths between 573 and 595 nm another broad peak is observed at the second overtone, $\sim 630 \text{ cm}^{-1}$. The intense, narrow peak at $\sim 68 \text{ cm}^{-1}$ and the small peak at $\sim 45 \text{ cm}^{-1}$ are acoustic modes. We attribute the small peak at $\sim 270 \text{ cm}^{-1}$ to two-phonon processes. The exciton-phonon coupling via the Fröhlich interaction concerns vibrational modes, and their overtones, that involve the electrostatic potential. Thus we will focus on the $l_p=0$ mode at 215 cm^{-1} and its overtones.¹¹ The other peaks in the Raman spectrum correspond to modes that either do not involve the electrostatic potential, or do not have overtones, and so will not be discussed further here. The Raman spectrum of PVA was recorded to ensure that none of the observed features in the Raman data are from the host material.

From previous measurements,⁵⁻⁷ we expect the resonance Raman excitation profile to follow the inhomogeneous distribution of the lowest exciton transition wavelengths. The Raman excitation profiles of the fundamental and first overtone of the $l_p=0$ phonon mode at 215 cm^{-1} are shown in Fig. 4. The values are normalized to the peak of the fundamental excitation profile at 580 nm. The ratio of fundamental to overtone intensity varies substantially across the excitation

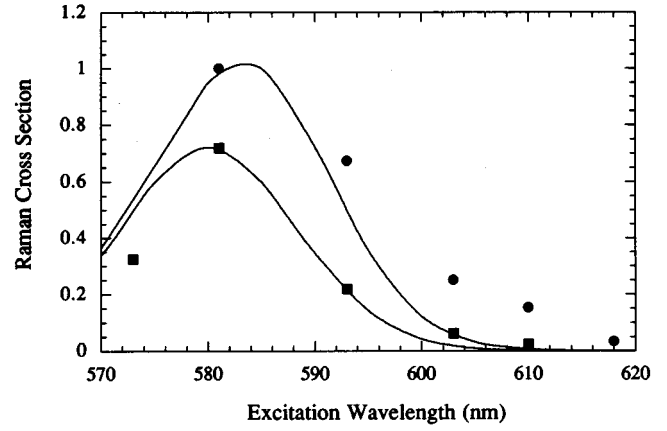


FIG. 4. Resonance Raman excitation profiles for 1.5-nm PbS nanocrystals at 4.2 K. The circles correspond to the fundamental vibrational mode at 215 cm^{-1} while the squares correspond to the first overtone. The solid lines are fits to the data using an offset harmonic oscillator model discussed in the text. The linewidth of the inhomogeneous distribution used in the fit was 500 cm^{-1} .

profile. This ratio decreases from 0.75 at 580 nm to 0.2 at 610 nm and is <0.05 (below the sensitivity of the experiment) at 618 nm. The solid lines are fits to the data using an offset harmonic oscillator model discussed below.

III. DISCUSSION

The coupling of the vibrational modes of a solid to the electronic states can be modeled as a displacement of the excited-state potential energy surface from the ground state along a single, harmonic normal-mode coordinate.^{12,16} Assuming a parabolic energy surface with the same curvature for both the excited and ground states, the displacement in the position dimension can be expressed as⁵

$$q_0 = 2\sqrt{\hbar/2\mu\omega_p} \Delta, \quad (3)$$

where μ is the reduced mass for an ionic pair. Using the above equation, Δ^2 and the Huang-Rhys parameter S are equivalent.

The Raman cross section for an n th order phonon process in a single nanocrystal is^{5,12}

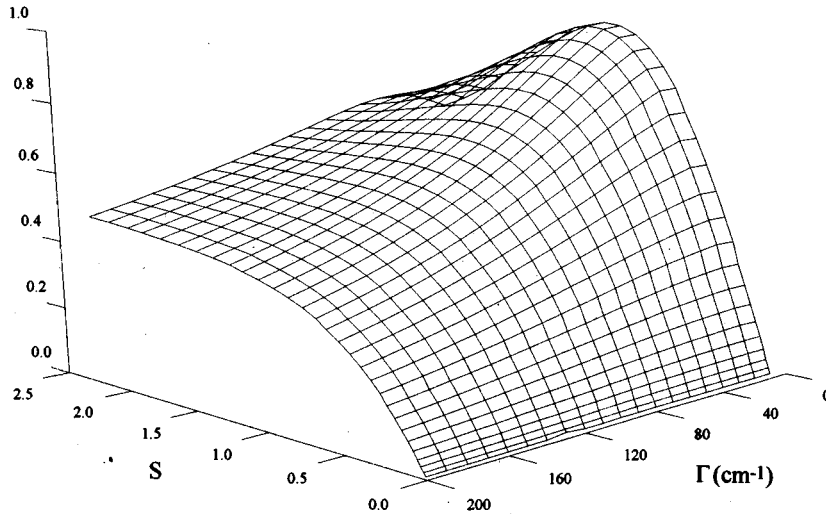
$$\sigma_n(E_g, \omega) = \mu_e^4 \sum_{j=0}^{\infty} \left| \sum_{m=0}^{\infty} \frac{\langle n+j|m\rangle \langle m|j\rangle}{E_g + (m-j)\hbar\omega_p - \hbar\omega + i\hbar\Gamma} \right|^2 \times e^{-j\hbar\omega_p/k_B T}, \quad (4)$$

where μ_e is the electronic transition dipole moment, $\hbar\omega$ is the incident photon energy, E_g is the energy of the lowest electronic transition, m denotes the intermediate vibrational state, T is the temperature, and Γ is the homogeneous linewidth. The overlap integral between the ground and excited states is equal to^{5,12}

$$\langle n|m\rangle = e^{-\Delta^2/2} \sqrt{n!m!} \Delta^{n-m} \sum_{j=0}^m \frac{(-\Delta^2)^j}{(m-j)!(n-m+j)!j!} \quad (5)$$

when $n \geq m$, and

Overtone/Fundamental



$$\langle m|n\rangle = (-1)^{n+m}\langle n|m\rangle.$$

The exciton transitions in a quantum dot are in general inhomogeneously broadened due to a distribution of particle sizes, and the particle-size distribution must be accounted for in the calculation of the total Raman cross section. The total Raman cross section is then

$$\sigma_n(\omega) = \int_{E_g} \sigma_n(E_g, \omega) \rho(E_g) dE_g, \quad (6)$$

where $\rho(E_g)$ is the distribution of nanocrystals. For calculational purposes, we assumed a Gaussian distribution for $\rho(E_g)$, which is a good fit to the lowest exciton transition in the absorption spectrum.

The above analysis shows that the ratio of the fundamental ($n=1$) to overtone ($n=2$) Raman intensities depends not only on S ($=\Delta^2$), but also on the homogeneous linewidth of the lowest electronic state Γ . With knowledge of the value of the dephasing rate, the value of S can be inferred from the resonance Raman spectrum. Figure 5 shows the calculated ratio of the Raman intensity of the first overtone to the fundamental, integrated over the nanocrystal size distribution, as a function of Γ and S for an excitation wavelength of 580 nm. Currently, we do not have an independent measurement of the electronic dephasing time $T_2=1/\Gamma$. However, values of Γ larger than 200 cm^{-1} will not accurately model the Raman data. Also, since the Raman intensity ratio is only a weak function of Γ (see Fig. 5) any resulting error in the inferred value of S is small.

The ratio of overtone to fundamental intensities decreases as the excitation wavelength is moved away from the peak of the lowest exciton transition, as shown in Fig. 6. Thus there is an apparent ambiguity regarding which value should be used to determine the exciton-phonon coupling. Shiang *et al.* also observed a large variation in this ratio across the Raman excitation profile of CdS nanocrystals.⁶ These workers suggest that the correct value of the ratio of overtone to fundamental intensities is obtained by either integrating over the Raman excitation profiles of the fundamental and overtone, or alternately using only the spectrum collected at the peak of the excitation profile.⁶ For an inhomogeneously broadened

FIG. 5. Calculated ratio of the overtone to fundamental Raman intensity vs the Huang-Rhys parameter S and the homogeneous linewidth of the first exciton transition Γ . The intensity ratio has been integrated over the nanocrystal size distribution. Note the origins of the three axes do not coincide.

exciton transition, the above calculation predicts that the overtone to fundamental ratio is greatest at the peak of the Raman excitation profile, and decreases away from the peak, in agreement with the trend we observe. A large variation in coupling strength across the lowest exciton transition could also explain the observed data. Since the particle size varies by only a few percent across the lowest exciton transition, this is unlikely. We fit the Raman excitation profile, and therefore also the ratio of overtone to fundamental intensity across the excitation profile, using the inhomogeneous linewidth and the exciton-phonon coupling strength as parameters. We find that good fits are obtained with an inhomogeneous linewidth of $400\text{--}700\text{ cm}^{-1}$, and the same value of S for all excitation wavelengths. The calculated ratios of overtone to fundamental intensity across the excitation profile agree very well with the measured values, as shown in Fig. 6. Attempts to fit the excitation profile using the inhomogeneous width obtained from the absorption spectrum ($\sim 1500\text{ cm}^{-1}$) produce a profile much wider than the measured one. Some uncertainty does exist in the values for the

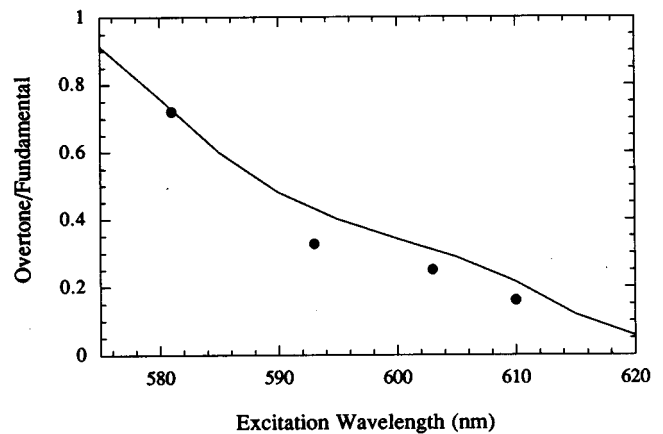


FIG. 6. Ratio of overtone to fundamental Raman intensity for the mode at 215 cm^{-1} . The circles are the experimental data and the solid line is a fit using the offset harmonic oscillators model. The linewidth of the inhomogeneous distribution used in the fit was 500 cm^{-1} .

inhomogeneous linewidths. The excitation wavelengths only cover about half of the Raman excitation profile, and there is some ambiguity as to the exact width of the lowest absorption peak (see Fig. 2). However, these uncertainties cannot account for the factor of 2 discrepancy between the inhomogeneous widths inferred from the Raman excitation profile and the absorption spectrum. Thus we conclude that the offset-harmonic-oscillator model accounts qualitatively, but not quantitatively, for the observed Raman excitation spectra. The lack of good quantitative agreement between the measured and calculated excitation profiles does not affect the inferred value of exciton-phonon coupling, since good fits to all of the data are obtained with a single value of S .

By fitting the resonance Raman excitation profile, and thus also the overtone to fundamental Raman intensity ratio across the excitation profile, we determine the value of the Huang-Rhys parameter S to be 0.7 for $\Gamma = 50 \text{ cm}^{-1}$ at 4.2 K. As mentioned above, the dependence of the value of S on Γ is weak. The best fit of 50 cm^{-1} for Γ is reasonable since values between 20 and 150 cm^{-1} have typically been observed for other semiconductor nanocrystals.¹⁷ Within experimental error, S does not vary as a function of temperature. The theoretical value of the Huang-Rhys parameter for a PbS nanocrystal with a 1.5-nm radius is 0.6×10^{-4} , 4 orders of magnitude smaller than the value obtained by experiment.

The strength of the exciton-phonon coupling reported for Cd(S,Se) nanocrystals is the same order of magnitude as that obtained for PbS nanocrystals, and is one order of magnitude greater than predicted by theory.² Similar values of the coupling strength for Cd(S,Se) nanocrystals have been measured with a variety of experimental techniques including resonant Raman spectroscopy,⁵⁻⁸ fluorescence line narrowing,⁹ and femtosecond photon echo.¹⁸ Nanocrystals made with II-VI materials have large coupling among the valence bands, and a weakly confined hole. Therefore, the intrinsic hole wave function is already somewhat localized, which creates a net charge imbalance in the nanocrystal. Cd(S,Se) nanocrystals are predicted to have exciton-phonon coupling two orders of magnitude larger than that of PbS nanocrystals (Fig. 1).

Calculations of exciton-phonon coupling for Cd(S,Se) nanocrystals that either contain an additional charge at the center,^{2,3} or use a donorlike exciton model,⁴ increase the resulting value of S by an order of magnitude, producing a result close to the experimentally determined value. This implies that the resonance Raman experiment samples electronic states that are vastly different from the intrinsic states of the nanocrystal. In addition, resonance Raman,^{5,6} fluorescence line narrowing,⁹ Stark effect,¹⁹ and luminescence^{20,21} experiments for Cd(S,Se) nanocrystals all indicate the existence of localized surface states. Thus an explanation for the observed coupling being one order of magnitude larger than the calculated coupling is that electronic states localized at the nanocrystal surface create a charge inhomogeneity, which strongly couples to the vibrational modes.^{6,9}

Refinements of the calculation of the exciton-phonon coupling for PbS nanocrystals (such as the use of finite potential barriers or accounting for Coulomb interactions) do not substantially change the result that the coupling will be weak. A calculated value of S as high as 0.7 can only be obtained when one charge carrier is highly localized in the nanocrystal,

similar to Cd(S,Se) nanocrystals. Evidence exists from transient nonlinear absorption measurements on PbS quantum dots of the type studied here that the intrinsic electronic state decays into an intermediate state after a few picoseconds.¹⁴ It is possible that the strong exciton-phonon coupling in PbS nanocrystals is due to an intermediate electronic state with one charge carrier trapped at the surface of the nanocrystal, and not the intrinsic electronic states.

Resonance Raman scattering is a time-integrated technique and therefore it is not sensitive to the dynamics of the exciton-phonon coupling. Evidence exists from transient differential absorption on CdSe nanocrystals that the intrinsic electronic states alone, with no contributions from surface states, are the initial excited states of the nanocrystal.²² Other evidence exists from Stark effect experiments¹⁹ and from femtosecond photon-echo experiments,¹⁸ also on CdSe nanocrystals, that the intrinsic electronic states have the hole partially trapped on the surface, which leads to a net dipole moment. While our Raman measurements indicate a large charge inhomogeneity in the PbS nanocrystal, these experiments cannot determine whether this state exists immediately after excitation or arises later after decay into a trapped state.

IV. CONCLUSION

We have examined the electron-phonon coupling strength in PbS nanocrystals. By analyzing resonant Raman scattering of PbS nanocrystals as a function of excitation wavelength, we find that the Huang-Rhys parameter $S \sim 0.7$. This is four orders of magnitude larger than the value we calculate from the intrinsic electronic and vibrational wave functions, but is consistent with that measured for other semiconductor nanocrystals. Similar to results for Cd(S,Se) nanocrystals, a calculation of the coupling strength that assumes that one charge carrier is localized produces a value for $S \sim 0.6$, which is close to the measured result. The results of our experiments support the proposition first made for Cd(S,Se) nanocrystals that the large exciton-phonon coupling is consistent with one charge carrier being localized at the surface.

The magnitude of exciton-phonon coupling and its dependence on nanocrystal radius are important issues in nanocrystal physics. Yet, it is clear that more work needs to be done in order to achieve a clear understanding of this phenomenon. We have just begun femtosecond photon-echo experiments on PbS nanocrystals. These experiments are designed to measure the strength of the electron-phonon coupling before the initial exciton state decays, and also to measure the electronic dephasing. There are some advantages to using nanocrystals of the lead salts rather than previously studied Cd(Se,S) materials to study exciton-phonon coupling. First, the intrinsic electron and hole wave functions are both delocalized and nearly identical. Thus, the coupling of vibrations to the intrinsic electronic states differs from that to electronic states involving a charge carrier trapped at the surface by four orders of magnitude. For Cd(S,Se) the intrinsic hole wave function is already somewhat localized due to its large effective mass, which creates a net charge imbalance in the nanocrystal. Thus a measurement of the coupling for PbS nanocrystals before the initial state decays should clearly indicate the nature of the electronic states immedi-

ately after excitation. Second, the experimentally determined values of the coupling for Cd(S,Se) could be affected by the many electronic states²³ in the vicinity of the lowest-energy peak in the absorption spectrum. However, the lowest-energy peak in the absorption spectrum of PbS nanocrystals is due to a single electronic state,¹⁰ making measurements of the exciton-phonon coupling more straightforward.

ACKNOWLEDGMENTS

The authors thank Inuk Kang and Yung Chun Lee for assistance with calculations, and Mick Thomas and John Silcox for high-resolution TEM measurements. T.D.K. acknowledges the support of the Optical Society of America.

-
- ¹S. Schmitt-Rink, D. A. B. Miller, and D. S. Chemla, *Phys. Rev. B* **35**, 8113 (1987).
- ²S. Nomura and T. Kobayashi, *Phys. Rev. B* **45**, 1305 (1992).
- ³Al. L. Efros, in *Phonons in Semiconductor Nanostructures*, edited by J. P. Leburton, J. Pascual, and C. S. Torres (Kluwer Academic Publishers, Dordrecht, Netherlands, 1993).
- ⁴J. C. Marini, B. Stebe, and E. Kartheuser, *Solid State Commun.* **87**, 435 (1993); J. C. Marini, B. Stebe, and E. Kartheuser, *Phys. Rev. B* **50**, 14 302 (1994).
- ⁵M. C. Klein, F. Hache, D. Ricard, and C. Flytzanis, *Phys. Rev. B* **42**, 11 123 (1990).
- ⁶J. J. Shiang, S. H. Risbud, and A. P. Alivisatos, *J. Chem. Phys.* **98**, 8432 (1993).
- ⁷A. P. Alivisatos, T. D. Harris, P. J. Carroll, M. L. Steigerwald, and L. E. Brus, *J. Chem. Phys.* **90**, 3463 (1989).
- ⁸G. Scamarcio, V. Spagnolo, G. Ventruti, M. Lugará, and G. C. Righini, *Phys. Rev. B* **53**, R10 489 (1996).
- ⁹M. Nirmal, C. B. Murray, and M. G. Bawendi, *Phys. Rev. B* **50**, 2293 (1994).
- ¹⁰I. Kang and F. W. Wise, *J. Opt. Soc. Am. B* (to be published).
- ¹¹T. D. Krauss, F. W. Wise, and D. B. Tanner, *Phys. Rev. Lett.* **76**, 1376 (1996). The radius of the PbS nanocrystals in this work was reported as 2 nm, but more recent measurements show that it is 1.5 nm. This does not change the conclusions of the paper.
- ¹²R. Merlin, G. Güntherodt, R. Humphreys, M. Cardona, R. Suryanarayanan, and F. Holtzberg, *Phys. Rev. B* **17**, 4951 (1978).
- ¹³M. T. Nenadovic, M. I. Comor, V. Vasic, and O. I. Micic, *J. Phys. Chem.* **94**, 6930 (1990).
- ¹⁴J. L. Machol, F. W. Wise, R. C. Patel, and D. B. Tanner, *Phys. Rev. B* **48**, 2819 (1993).
- ¹⁵R. Loudon, *J. Phys. (Paris)* **26**, 677 (1965).
- ¹⁶M. L. Williams and J. Smit, *Solid State Commun.* **8**, 2009 (1970).
- ¹⁷It is interesting to note that T_2 can vary by several orders of magnitude across an inhomogeneously broadened line when excitons can dephase by scattering from each other. This is the case for excitons in two-dimensional structures, for example. However, there is no scattering among excitons in different quantum dots.
- ¹⁸D. M. Middleman, R. W. Schoenlein, J. J. Shiang, V. L. Colvin, A. P. Alivisatos, and C. V. Shank, *Phys. Rev. B* **49**, 14 435 (1994).
- ¹⁹V. L. Colvin, K. L. Cunningham, and A. P. Alivisatos, *J. Chem. Phys.* **101**, 7122 (1994).
- ²⁰F. Hache, M. C. Klein, D. Ricard, and C. Flytzanis, *J. Opt. Soc. Am. B* **8**, 1802 (1991).
- ²¹M. G. Bawendi, P. J. Carroll, W. L. Wilson, and L. E. Brus, *J. Chem. Phys.* **96**, 946 (1992).
- ²²D. J. Norris and M. G. Bawendi, *J. Chem. Phys.* **103**, 5260 (1995).
- ²³A. I. Ekimov, F. Hache, M. C. Schanne-Klein, D. Ricard, C. Flytzanis, I. A. Kudryavtsev, T. V. Yazeva, A. V. Rodina, and Al. L. Efros, *J. Opt. Soc. Am. B* **10**, 100 (1993).